

## Biosorption of antimony using tea leaves and tea fibers (*Camellia sinensis*) as adsorbents: thermodynamics, isotherm, and kinetics

EMMANUEL E. ETIM\*, SHEDRACH YAKUBU, RICHARD OKAFOR, BULUS BAKO

Department of Chemical Sciences, Federal University Wukari, Taraba State, Nigeria

\*Corresponding author: emmaetim@gmail.com

Received:  
08.08.2024

Accepted:  
21.06.2024

Published:  
04.07.2024

### Abstract

Rapid industrial development causes environmental contamination of land, water, and air with heavy metals which pose a significant threat to human survival. This study aims to remove antimony from wastewater using tea leaves and tea fiber (*Camellia sinensis*) as an adsorbent to curb the environmental decay posed by industrialization. The FTIR study presents significant vibration frequencies that correspond to  $-OH$ ,  $C-H$ , and  $C=O$  in both the leaves and fibers which impact the adsorption. The adsorption study was performed by the batch adsorption method, varying different parameters including pH, adsorbent dosage, temperature, initial concentration, and contact time to find best-suited conditions for the removal of antimony from aqueous media. The results show an equilibrium condition at pH 5 and 30 minutes for both tea leaves and fibers whereas for tea leaves the equilibrium concentration was obtained at a dosage of 2g, and 3g for the fiber. From the adsorption model, the sorption of antimony by tea leaves follows the Langmuir model ( $R^2 = 0.783$ ), whereas that of tea fiber follows Freundlich ( $R^2 = 0.827$ ). From Kinetic studies, the sorption of antimony by both plant parts follows second-order kinetics with approximate  $R^2$  values of 1. From the adsorption capacity, it is no exaggeration to consider tea leaves and fibers as an excellent biosorbent for the sorption of antimony.

**Keywords:** antimony adsorption, tea leaves and fibers, kinetics, thermodynamics, isotherm

### INTRODUCTION

Earth-crust, including land, atmosphere, and water bodies, is contaminated by anthropogenic activities like industrial effluents, mining, explosives, metal plating, domestic effluents, leaching, and garbage run-offs [1]. These environmental pollutants contain several heavy metal ions and the danger associated with the presence of these heavy metals has been attributed to bioconcentration and bioaccumulation in the food chain [2] and transported to several locations usually by water [3]. Industrialization has rapidly increased the demand for the exploitation of natural resources and exacerbated environmental pollution, particularly in antimony deposition into water bodies over the past century [4]. Heavy metal pollution, a growing global concern, is causing significant environmental damage due to various pollutants including inorganic ions, organic pollutants, organo metallic compounds, radioactive isotopes, gaseous pollutants, and nanoparticles.

Heavy metals as described by Barrera et al., [5] are elements whose density is equal to or greater than  $6.0 \text{ g/cm}^3$  e.g. Lead (Pb), mercury (Hg), cadmium (Cd), and arsenic (As). They have long been used by man as building materials, as medicine, as pigments, or as additives for petrol [6, 7]. Researchers later proved that heavy metals generally pose a great deal of problems to mankind due to their presence in the environment at concentrations above the threshold [8]. Heavy metal pollution is a global environmental issue causing health complications like lead poisoning, as it is toxic, indestructible, and bioaccumulates, affecting various systems [9]. Also, excess ingestion of zinc can lead to microcytosis, impaired immune response, neutropenia, and hypocupremia, [10].

Biosorption of heavy metal is a common practice in industries to reduce environmental pollution and contamination, reported as a low-cost and efficient method by researchers [11, 12]. A good number

of agricultural wastes have been investigated for potential biosorption efficiency. Lately, Saleh [13] reported that adsorption is one of the most suitable techniques for the removal of antimony from wastewater. Antimony biosorption activity of grapefruit peel, peapod shelling, green bean husk wheat straw, black gram husk, rice straw, and husk were investigated by Iqbal *et al.*, [14]; that of lichen *Physcia tribacia* studied by [15]; and, Hasan *et al.* [16] revealed excellent Sb(V) removal efficiency of orange peels treated with acetic acid. The Proposed mechanism for biosorption depends on the interactions between the metallic cations and the anions contained in the biomass [17]. Adsorption has been studied using various models, such as Langmuir and Freundlich isotherm, to gain a better understanding of its nature [18]. The thermodynamic consequences of the biosorption process highlight exothermic and endothermic aspects which indicate the suitability of nonliving biomass for various adsorption studies. The surface modification techniques reported by Yakubu *et al.*, [19] for biomass surface functionalization increase the sorption capacity. The common chemical modification methods are acid or alkali treatment and cross-linking with glutaraldehyde and epichlorohydrin. This study explores the use of *Camellia sinensis* biomass as an adsorbent for heavy metal removal from contaminated aqueous solutions. It highlights the potential of converting tea leaves and fibers into biosorbents, reducing waste and pollution while promoting a safe aqua environment.

## **MATERIALS AND METHODS**

The reagents used in the experiments were Sb<sub>2</sub>O<sub>3</sub> (Analytical grade), HCl (ECO-CHEM Ltd 69% Technical Grade), and NaOH (98% ACL Labscan). A stock solution of antimony pentaoxide of about 0.1 M was dissolved in distilled water from which serial dilutions were made for concentrations of 20 mg/L, 30 mg/L, 40 mg/L, and 50 mg/L. 0.1 M solution of HCl and 0.1 M NaOH was also prepared in distilled water. Fourier transformed infrared spectroscopy (Happ-Genezel) was used for functional group analysis and Atomic Adsorption Spectroscopy AA500 AAS (PG Instruments) for residual metal concentrations after adsorption.

### *Preparation of adsorbent*

Both tea leaves and tea fiber (*Camellia sinensis*) used for this experiment were collected from Kakara High Land Tea, Sarduna L.G.A of Taraba State. The leaves were washed and rinsed, sun dried for 7 days, pulverized, sieved, and stored in an airtight polyethylene bag for analysis. The dried tea fiber was also pulverized and sieved [20].

### *Adsorption studies*

Batch adsorption studies were carried out to obtain both rates of adsorption and equilibrium data. This was performed by varying concentration, adsorbent dosage, contact time, pH level, and temperature.

### *Effect of Biosorbent dosage*

About 1 g, 2 g, 3 g, and 4 g of the adsorbent was weighed into different conical flasks. 50 cm<sup>3</sup> of metal solution was measured into each of the conical flasks and labeled. The flasks were corked, and the mixture was agitated with the aid of a shaker for 1 hour to attain equilibrium, the slurries were then filtered using Whatman filter paper and a plastic funnel, the filtrates were kept in well-labeled containers and thereafter the concentrations of the resulting filtrate were determined using atomic absorption spectrometer [21, 22].

### *Effect of time*

About 1 g of biosorbent was suspended in different conical flasks containing 50 cm<sup>3</sup> 40 mg/L of antimony metal solution. Each beaker was agitated on an electrical shaker/rotatory mixer at 30 rpm and the time difference between each beaker was 10 minutes, 20 minutes, 30 minutes, and 40 minutes. A temperature of 25 °C, pH of 6, and concentration of metal 0.1 M were kept constant. The solutes were extracted, centrifuged at 4000 rpm for 3 minutes, separated from the biosorbent, and then analyzed using an atomic absorption spectrometer [21÷23].

### *Effect of Initial Concentration*

Approximately 50 cm<sup>3</sup> each of metal solution, containing different concentrations; 20 mg/L, 30 mg/L, 40 mg/L, and 50 mg/L were measured into different conical flasks. 1 g of the biosorbent was dispersed onto each of them, the flasks were corked, and the mixture was agitated with the aid of a shaker for 1 hour to attain equilibrium, the slurries were then filtered using Whatman filter paper and a plastic funnel. The filtrates were then kept in well-labeled containers and thereafter the concentrations of the resulting filtrates were determined using an atomic adsorption spectrometer [22, 24].

### *Effect of pH*

For the effect of pH on the biosorption of Antimony (Sb), experiments were conducted at 25°C by contacting 1 g of the tea leaves and tea fiber with 50 cm<sup>3</sup> of 40 mg/L antimony solution in a conical flask. The pH of each of the solutions was adjusted to the desired value with 0.1 M sodium hydroxide and or 0.1 M Hydrochloric acid. The study analyzed antimony concentration in conical flasks at different pH values, and decanted biomass, and analyzed residual antimony concentration in triplicates using an AAS machine [25÷28]. The effect of pH on the biosorption of metal ions was carried out within the range that does not influence the precipitation of the metal [29].

### *Effect of temperature*

About 50 cm<sup>3</sup> of 40 mg/L of the antimony metal solution was measured into four different conical flasks which were adjusted on a temperature scale of 313 K, 323 K, 333K, and 343 K. 1 g of the adsorbent was then weighed and poured into each flask. The slurries were shaken for 1 hour, filtered using Whatman paper and a funnel, and the concentration of the filtrates was determined using an Atomic Adsorption spectrometer [21, 22].

### *Estimation of Metal Uptake*

The equilibrium metal uptake  $q_e$  and the adsorption efficiency in the percentage of the biomass were calculated according to equations 1 and 2:

$$q_e = \frac{(C_o - C_e)}{m} v, \quad (1)$$

$$\% \text{ efficiency} = \frac{(C_o - C_e)}{C_o} \times 100, \quad (2)$$

where  $q_e$  is the metal ions uptake at equilibrium (mg/g),  $V$  is the volume of the metal solution used (L),  $C_o$  is the initial concentration of a metal ions in solution (mg/L),  $C_e$  is the final concentration of a metal ion in solution at equilibrium (mg/L), and  $m$  is the mass of biosorbent (g).

### *Characterization of adsorbent: adsorption kinetics*

Kinetics involves the study of the rate of chemical reactions or processes and facilitates an understanding of the factors that influence these rates. It is important to monitor the experimental conditions that influence the speed of a chemical reaction in its race toward equilibrium. These kinetics provide information about the possible mechanism of adsorption. In addition, the different transition forms until the final adsorbent complex are revealed. The data obtained is used to develop appropriate mathematical models to describe the interaction. The adsorption mechanism of Antimony onto the tea leaves and tea fiber was studied using first order and second-order kinetic equations [30].

### *Pseudo-first order kinetics model*

The first-order rate expression of the Langeron model is expressed in equation 3:

$$\frac{\partial q_t}{\partial t} = K_1(q_e - q_t) \quad (3)$$

The integrated rate law after application of the initial concentration at  $q_t = 0$  and  $t = 0$ ; becomes a linear equation given by equation 4:

$$\log(q_e - q_t) = \log q_e - \frac{k_1}{2.303} t \quad (4)$$

where:  $q_e$  is the quantity of metal uptake at equilibrium (mg/g),  $q_t$  is the quantity of metal uptake at time  $t$ . If the pseudo-first order is applicable, a plot of  $\log(q_e - q_t)$  versus  $t$  should yield a linear

connection. The slope and intercept of the curve can be used to derive the constant  $k_1$  and projected, respectively [31].

#### *Pseudo-second order kinetics model*

The first order kinetics model gives only  $k_1$  and  $q_e$  cannot be estimated using this model, the applicability of the second order kinetics must be tested for the estimation of  $q_e$  with the rate equation is given by:

$$\frac{\partial q_t}{\partial t} = K_2(q_e - q_t)^2 \quad (5)$$

Integrated rate expression for second order kinetic model is presented in equation 6:

$$\frac{1}{q_t} = \frac{1}{k_2 q_e^2} + \frac{1}{q_e} t \quad (6)$$

where:  $k_2$  (mg/g.min) is the rate constant of the second-order equation,  $q_t$  (mg/g) is the metal adsorbed at time  $t$  (min), and  $q_e$  is the metal adsorbed at equilibrium (mg/g). A plot of  $t/q_e$  versus  $t$  should be given a linear relationship which allows the computation of the second-order rate constant  $k_2$  and  $q_e$ . The second-order model assumes that the rate-limiting step may be chemical adsorption involving valence forces through the sharing or ion exchange of electrons between the adsorbent and adsorbate [32].

#### *Equilibrium Isotherm Model*

The analysis of isotherm data is crucial for developing accurate equations for design and optimization. The most common isotherms in solid-liquid systems are theoretical equilibrium isotherms like Langmuir and Freundlich [33].

#### *Langmuir Adsorption Isotherm*

The Langmuir adsorption isotherm, also known as the ideal localized monolayer model, is a theoretical framework that studies the adsorption of gases on solid surfaces [34]. Adsorption of adsorbate into an adsorbent requires three assumptions: contact with strongly attracted adsorbent surface, monolayer adsorption, and specific sites for solute adsorption. The Langmuir isotherm equation is presented in equation 7.

$$q_e = \frac{Q_0 K_L C_e}{1 + K_L C_e} \quad (7)$$

Langmuir adsorption parameters were determined by transforming the Langmuir equation into linear form (equation 8).

$$\frac{1}{q_e} = \frac{1}{Q_0} + \frac{1}{Q_0 K_L C_e} \quad (8)$$

where:  $C_e$  is the equilibrium concentration of adsorbate (mg/L),  $q_e$  is the amount of metal adsorbed per gram of the adsorbent at equilibrium (mg/g),  $Q_0$  is maximum monolayer coverage capacity (mg/g),  $K_L$  is the Langmuir isotherm constant (L/mg). The values of  $Q_0$  and  $K_L$  were computed from the slope and intercept of the Langmuir plot of  $\frac{1}{q_e}$  versus  $\frac{1}{C_e}$ .

The equilibrium parameter  $R_L$ , is a dimensionless constant referred to as the separation factor (equation 9).

$$R_L = \frac{1}{1 + (1 + K_L \times C_0)} \quad (9)$$

where:  $C_0$  is the initial concentration,  $K_L$  is the constant related to the energy of adsorption (Langmuir),  $R_L$  value indicates the adsorption nature. It is either unfavorable ( $R_L > 1$ ), linear ( $R_L = 1$ ), favourable ( $0 < R_L < 1$ ) and irreversible ( $R_L = 0$ ).

#### *Freundlich adsorption isotherm*

Regarding Freundlich adsorption isotherm, it is assumed that the stronger bonding sites are occupied first, and the binding strength decreases with increasing degree of site occupation. This isotherm are used to study the heterogeneity and surface energy. The empirical equation proposed by Freundlich is presented in equation 10:

$$q_e = K_f C_e^{\frac{1}{n}} \quad (10)$$

where:  $K_f$  and  $n$  are coefficients,  $q_e$  is the weight adsorbed per unit weight of adsorbent,  $C_e$  is the equilibrium concentration of the metal solution. Taking logarithm and rearranging, the following equation results:

$$\log q_e = \log K_f + \frac{1}{n} \log C_e \quad (11)$$

The constant  $K_f$  is an approximate indicator of adsorption capacity, while  $1/n$  is a function of the strength of adsorption in the adsorption process [35].

If  $n = 1$  then the partition between the two phases are independent of the concentration. If the value of  $1/n$  is below one it indicates normal adsorption [36]. When  $1/n$  is more than one, cooperative adsorption takes place [36]. As a result, when the system's temperature rises, changes in the constants  $K_f$  and  $n$  indicate slow adsorption, which calls for higher pressure to enhance sorption saturation at the surface. When determining the kinetics and isotherm models of the sorbent-sorbate process, the  $K_f$  and  $n$  parameters play a crucial role [37, 38]. The  $1/n$  values have a significant influence on the heterogeneity of the system defined by both linear transform equations and linear least squares. When  $1/n = 1$ , this expression reduces to a linear adsorption isotherm. A favourable sorption process is indicated if  $n$  is between one and ten.

### *Thermodynamic studies*

In environmental engineering practice, both energy and entropy factors must be considered to determine which process will occur spontaneously [39]. The thermodynamic parameters were obtained by varying the temperature conditions while keeping other variables constant including metal concentration, pH, adsorbent dose, and contact time. The apparent equilibrium constant ( $K_c$ ) of the biosorption is defined in equation 12:

$$K_c = \frac{q_e}{C_e} \quad (12)$$

where  $q_e$  is the concentration of silver on the adsorbent (mg/g) and  $C_e$  is the residual silver concentration at equilibrium (mg/L). In this case, the activity should be used instead of concentration to obtain the standard thermodynamic equilibrium constant ( $k_c$ ) of the absorption system [40].

The values of the thermodynamic parameters such as  $\Delta G^\circ$ ,  $\Delta H^\circ$ , and  $\Delta S^\circ$ , can be calculated using the expression presented in equation 13. The Gibb's free energy of the absorption process is calculated [35].

$$\Delta G^\circ = -RT \ln K_c \quad (13)$$

Where  $\Delta G^\circ$  represents the standard Gibb's free energy change for the adsorption (J/mol),  $R$  represents the universal gas constant (8.314 J/mol/K) and  $T$  represents the temperature (K). The plot of  $\ln K_c$  versus  $1/T$  gives a straight line with the slope and the intercept giving values  $\Delta H^\circ$ , and  $\Delta S^\circ$ . These values could be used to compute  $\Delta G^\circ$  from Gibb's relation (equation 14).

$$\Delta G^\circ = \Delta H^\circ - T\Delta S^\circ \quad (14)$$

Positive change in enthalpy ( $\Delta H^\circ$ ) implies that the adsorption is an endothermic process, but positive change in entropy ( $\Delta S^\circ$ ) reflects enhanced randomness at the solid/ solution interface.

## **RESULT AND DISCUSSION**

### *FTIR analysis*

FTIR is used to analyze vibrational frequencies of functional groups, revealing their molecular structure. Non-zero dipole moment in these groups influences chemisorption of metallic pollutants by biomass. Table 1 presents the difference in functional groups for tea leaves and tea fibers.

The FTIR results of tea leaves exhibit N-H at  $3697.5 \text{ cm}^{-1}$  indicating the presence of primary amine; O-H band at  $3615.6 \text{ cm}^{-1}$  corresponding to alcohol, carbohydrate, proteins, and phenols; C-H band at  $2918.5 \text{ cm}^{-1}$  an indicative of alkane; P- band at  $2322.1 \text{ cm}^{-1}$  corresponding to phosphine and C=O signaling an aromatic ketone. The presence of primary amine was fully confirmed with the band at  $1606.6 \text{ cm}^{-1}$ , also the band at  $1364.2 \text{ cm}^{-1}$  is an indicative aromatic amine; a band at  $1233.7 \text{ cm}^{-1}$  signaled the carboxylic acid and  $1010.1 \text{ cm}^{-1}$  shows the presence of primary alcohol or/and ether [41].

**Table 1. FTIR analysis for tea leaves and tea fiber**

Tea leaves			Tea fibers		
Peak wavelength	Bond type	Functional group	Peak wavelength	Bond type	Functional group
3697.5	N-H	Primary amine	3276.2	O-H	Carbohydrate; protein; phenol
3615.6	O-H	Carbohydrate; protein; alcohol	2918.5	C-H	Alkane
2918.5	C-H	Alkane	1625.1	-C=O	Amide band I
2322.1	P-	Phosphine	1513.1	-C=O	Carboxylic acid
1729.5	C=O	Aromatic ketone	1513.8	C-N	Amide band III
1606.5	N-H	Primary amine	1144.2	C-O	Secondary alcohol
1461.1	-C=O	Inorganic carbonate	1017.6	R-O-R	Ether
1364.2	C-N	Aromatic amine			
1233.7	R-COOH	Carboxylic acid			
1010.1	C-O	Primary alcohol			

The FTIR results of tea fiber, on the other hand, exhibit an O-H stretch band at 3276.3  $\text{cm}^{-1}$  corresponding to alcohol, carbohydrate, proteins, and phenols; C-H band at 2918.5  $\text{cm}^{-1}$  indicating an Alkane; a  $-\text{C}=\text{O}$  band at 1625.1  $\text{cm}^{-1}$  correspond to the amide; while a C-O band at 1144.2  $\text{cm}^{-1}$  correspond to secondary alcohol and C-O band at 1017.6 indicates an ether or/and primary alcohol. The spectrum explains that some peaks were shifted or disappeared, and new ones formed. These changes observed indicate the tendency of chemical adsorption.

#### Adsorption studies: pH effect

Figure 1 presents the plots of the effect of pH on the adsorption of both tea leaves and tea fibers. From the graph, it was observed that there was a decrease in adsorption as the acidity decreased from pH of three to five followed by a steady increase as the acidity further decreased for tea leaves. The tea fiber's adsorption efficiency increased with pH increase from three to five, then decreased as pH shifted towards alkalinity, establishing an equilibrium concentration at pH 5. At low pH values, metals compete with excess  $\text{H}^+$  ions for adsorption on sorbent surfaces, reducing removal and biosorption efficiency. Raised pH increases adsorption due to  $-\text{OH}$  group attraction [42].

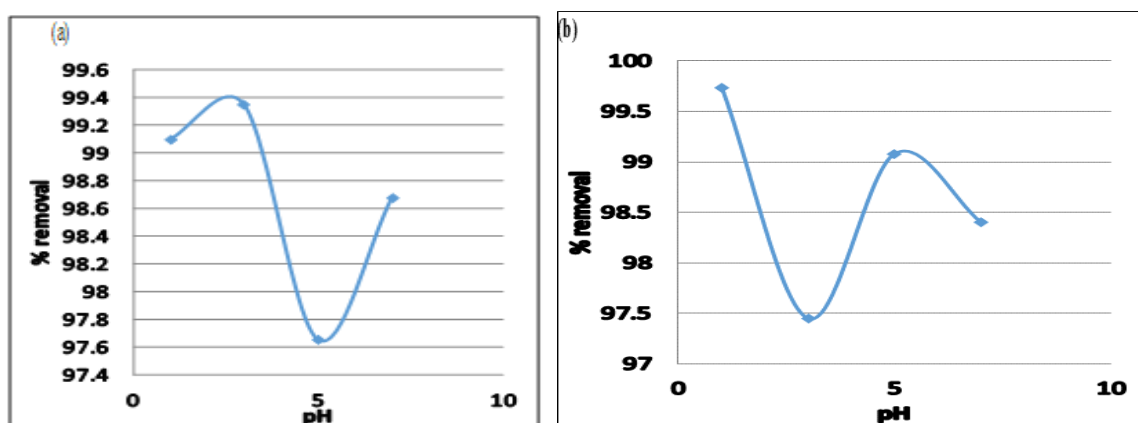


**Fig. 1.** Effect of pH of the sorption of antimony by tea leaves (a) and tea fibers (b) at 40 mg/L Antimony / 1 g bio sorbents

#### Effect of adsorbent dosage

The experiment results on the effect of adsorbent dosage in Figure 2 shows respectively that equilibrium was attained at an adsorbent dosage of 2.0 and 3.0 g for tea leaves and tea fiber respectively. Beyond this equilibrium condition, the adsorption efficiency dropped below the

equilibrium concentration. This indicates that the adsorption of antimony unto both tea leaves and tea fiber increases steadily and reaches a maximum, then desorption sets in. The biosorption efficiency of tea fiber decreases between 1 and 2 g dosage of biosorbent due to lower available binding sites or functional groups to the initial concentration of metallic pollutants, as fewer pollutants exhaust the limited binding sites.

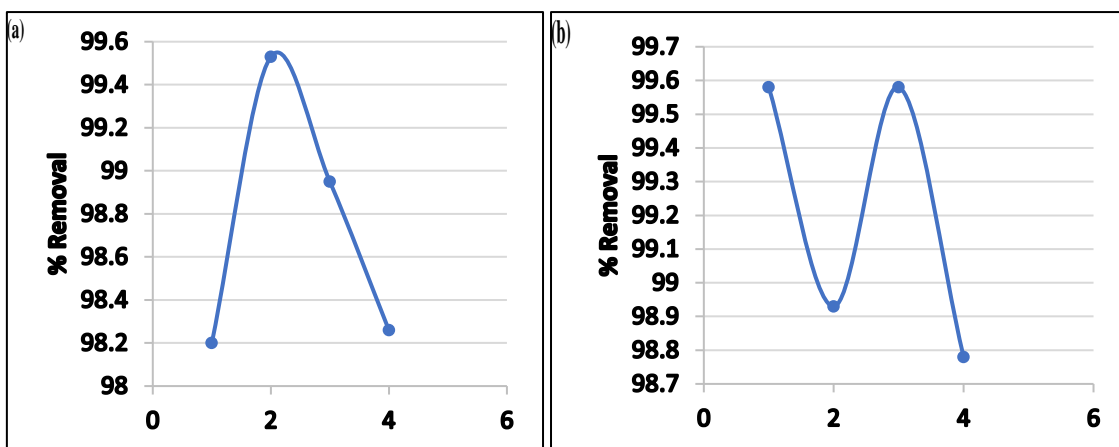


**Fig. 2.** Effect of dosage (g) of the sorption of antimony by tea leaves (a) and tea fibers (b), in %

*Effect of initial concentration*

The effect of the initial concentration of antimony in the aqueous solution shows an increase in % removal with a decrease in concentration for tea leaves and the tea fiber shows a steady decrease in % removal with increasing metallic ion concentration as presented in the plots of Figure 3(a, b). The equilibrium concentration for both the tea leaves and tea fibers to the effect of initial concentration were obtained at a dosage of 40 and 30 mg/L respectively.

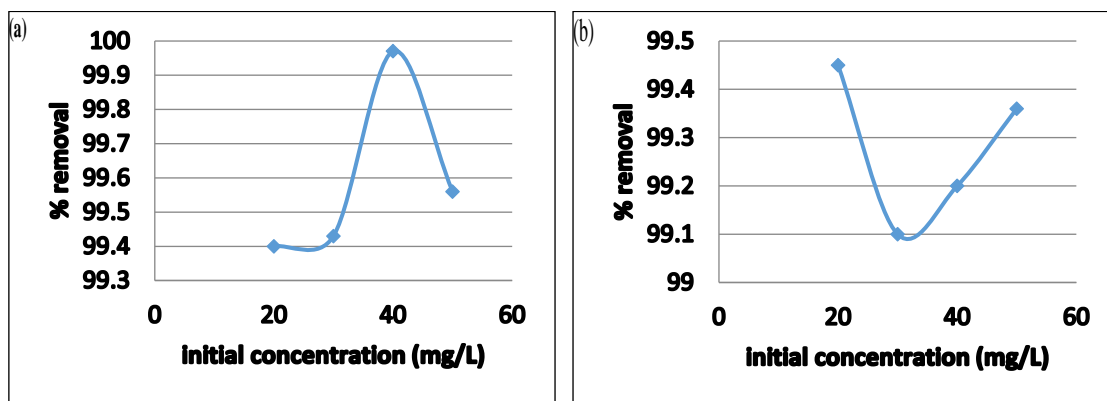


**Fig. 3.** Effect of initial concentration (mg/L) of antimony on the sorption efficiency of tea leaves (a) and tea fibers (b), in %

*Effect of temperature*

The study reveals that temperature affects the adsorption of antimony on tea leaves and tea fiber, with an increase in temperature causing a decrease in adsorption captured in figure 4 (a, b). This indicates that adsorption reactions are normally exothermic. For the tea leaves (figure 4a) between the temperatures of 313 and 333 K, the adsorption efficiency remains almost stable, attaining an equilibrium at about 333 after which a steep decline in the adsorption efficiency was observed as the temperature increases up to 343 K. For the tea fiber, the reverse was the case where there was a steep decline in the adsorption efficiency between 313 and 333 k and maintaining an almost stable condition above these temperatures. In essence, increasing temperature decreases the adsorption efficiency of the biosorption of antimony by tea leaves and tea fibers respectively.

### Effect of contact time

Time is a crucial parameter in biosorption studies, as it provides insight into kinetics and rate of process, essential for efficiency in industrial applications. The effect of contact time on batch adsorption for both tea leaves and tea fiber show that adsorption decreases between 15 and 20 minutes and then increases steadily between 20 minutes to 30 minutes (figure 4 b, c). The % removal of the metal by the biosorbent then starts decreasing again with an increase in time up to 40 minutes. This implies that equilibrium time was attained at 30 minutes since adsorption decreases afterward. The adsorption process was found to be very rapid initially and a very large fraction of the total concentration of metal was removed in the first 30 minutes.

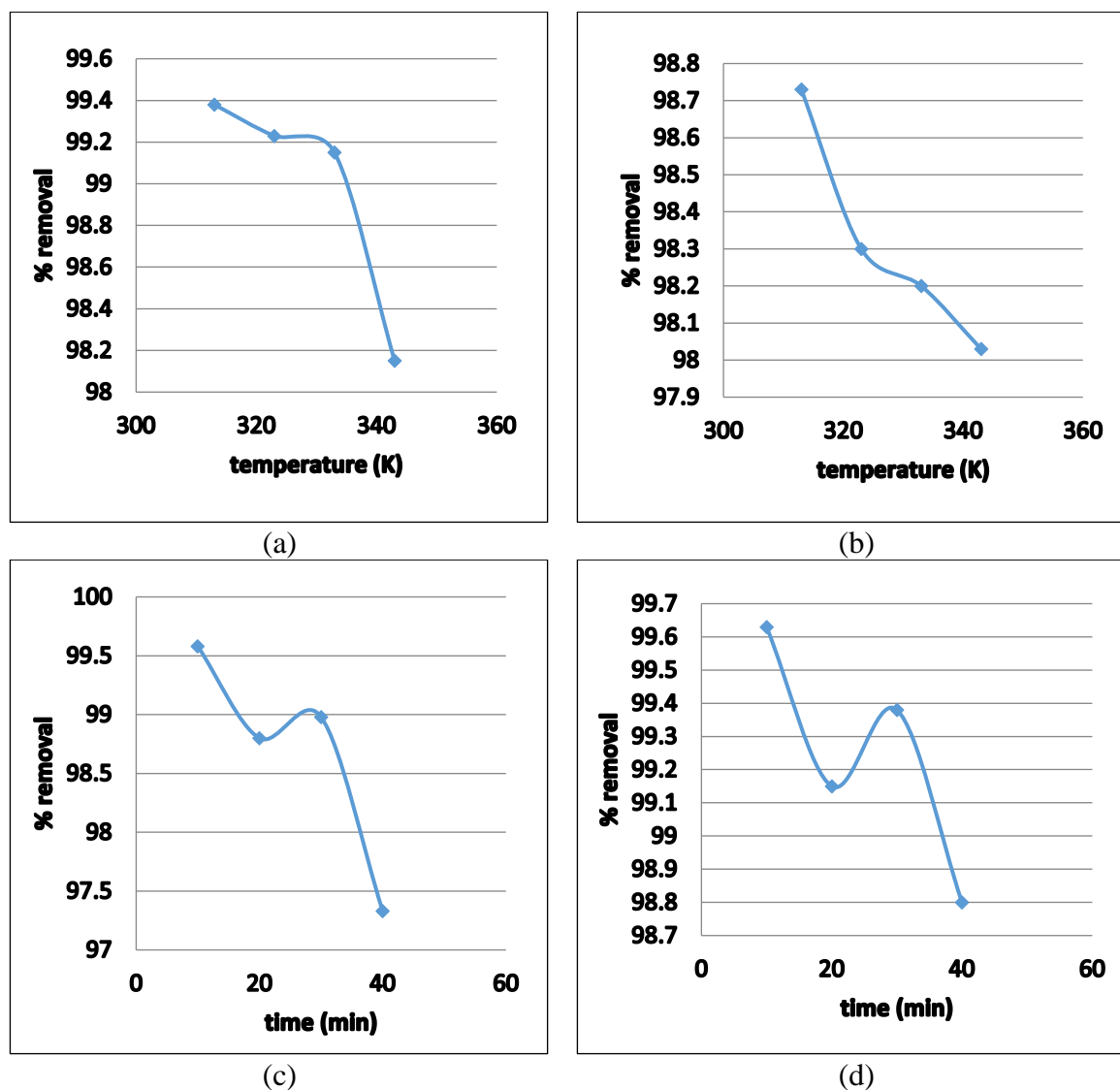


**Fig. 4.** Effect of temperatures (a, b) and effect of time (c, d) on the sorption efficiency of tea leaves (a, c) and tea fibers (b, d) at 40 mg/L Antimony/1 g biosorbents

### Adsorption isotherm

Adsorption isotherms describe the relationship between bulk adsorbate concentration and adsorbed amount at the interface, assuming all adsorption sites are equivalent and particle binding ability is independent of adjacent sites [39, 43]. The research utilized Langmuir and Freundlich isotherm models for process simulation to enhance understanding of the adsorption isotherm of antimony. For the Langmuir model, the regression correlation coefficient ( $R^2$ ) for both tea leaves and tea fiber was found to be 0.783 and 0.252 respectively and that of the Freundlich was 0.3607 and 0.8265 for both tea leaves and tea fiber respectively (figure 5). This implies that the equilibrium data agrees well with

Langmuir better than Freundlich which assumes that a monolayer is formed and the uniform energies of adsorption onto the tea leaves and tea fiber and that no trans-migration of antimony on the adjacent binding sites, [44].

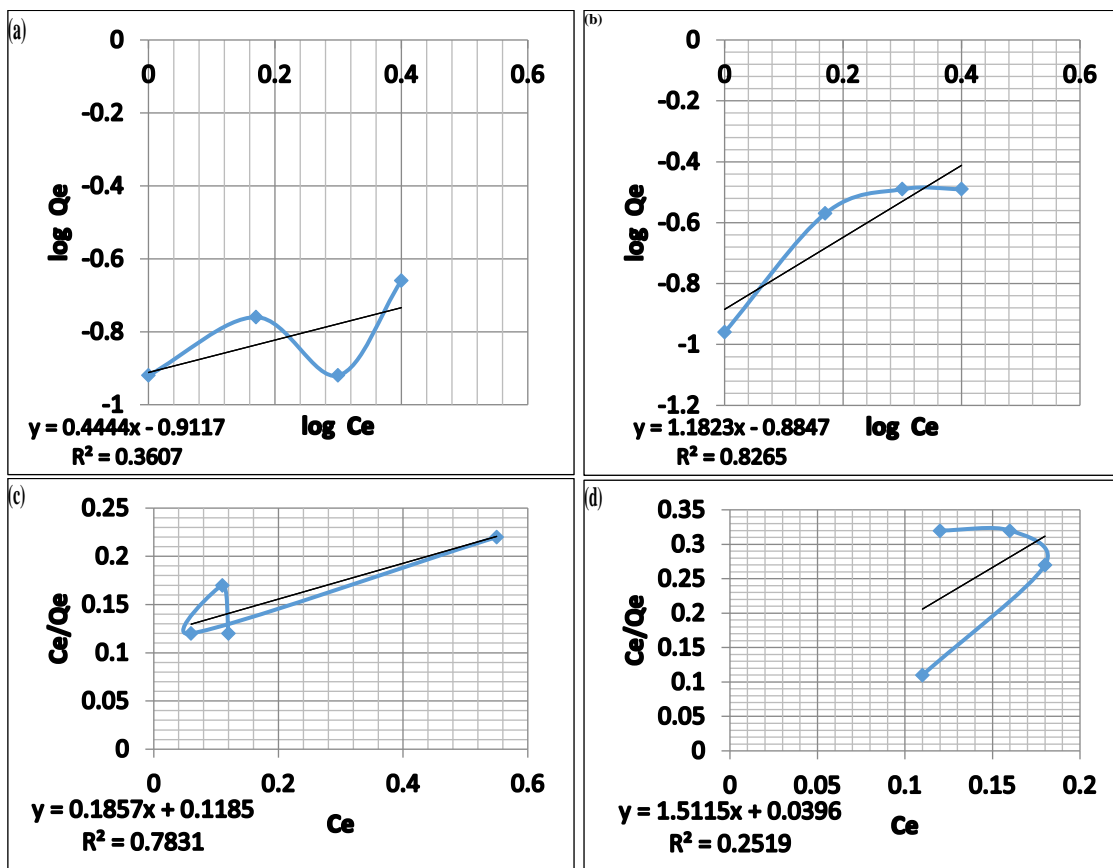


Fig. 5. Freundlich isotherm plot (a, b) and Langmuir adsorption isotherm plot (c, d) for tea leaves (a, c) and tea fibers (b, d)

Table 2. Langmuir and Freundlich result for tea leaves and fibers

	Langmuir isotherm				Freundlich isotherm			
	Q <sub>o</sub> (mg/g)	K <sub>L</sub> (L/mg)	RL	R <sup>2</sup>	1/n	n	K <sub>f</sub> (mg/g)	R <sup>2</sup>
Tea leaves	0.1857	0.1185	6.74	0.783	0.444	2.252	-0.0401	0.3607
Tea fiber	1.5115	0.0396	3.584	0.2519	1.182	0.843	-0.0532	0.8265

### Thermodynamics

The thermodynamic behavior of the biosorption of Sb(II) on the biomass can be fully understood by calculating the thermodynamic parameters including the enthalpy and entropy from the slope and intercept of a plot of  $\ln k_c$  versus  $1/T$  as shown in Figure 6 (a, b) for the tea leaves and tea fiber respectively (tables 3, 4).

Table 3. Percentage removal related to the temperatures

Adsorbent	Temp, K	1/T*10 <sup>-3</sup>	Ce(mg/L)	Qe(mg/L)	Kc(g/L)	ln kc	%removal
Tea leaves	313	3.20	0.250	1.9875	7.95	2.07	99.38
	323	3.10	0.310	1.9845	6.40	1.86	99.23
	333	3.00	0.340	1.983	5.83	1.76	99.15
	343	3.90	0.740	1.963	2.65	0.97	98.15
Tea fibers	313	3.20	0.500	1.975	3.95	1.37	98.75
	323	3.10	0.68	1.966	2.89	1.069	8.30
	333	3.00	0.720	1.964	2.73	1.00	98.20
	343	3.90	0.790	1.196	1.51	0.41	98.03

The biosorption of Sb(II) ion on tea leaves and fiber showed an endothermic enthalpy change, increasing randomness at the solid/solution interface. The Gibbs free energy change indicated spontaneity, confirming the process's feasibility and spontaneous nature.

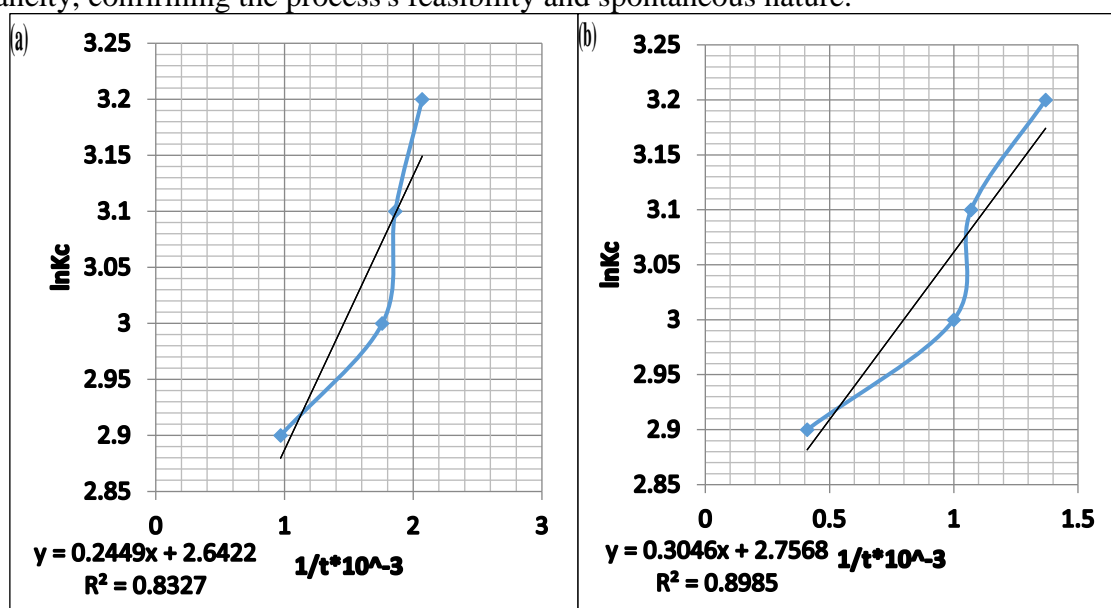


Fig. 6. Thermodynamic studies for tea leaves (a) and tea fibers (b).

Table 4. Thermodynamic parameter

Temperatures K	Tea Leaves Adsorbent		
	$\Delta G^\circ$ (KJ/mol)	$\Delta H^\circ$ (KJ/mol)	$\Delta S^\circ$ (KJ/mol)
313	-826.764	0.2449	2.6422
323	-853.186		
333	-879.608		
343	-906.029		
Temperatures K	Tea Fibers Adsorbent		
	$\Delta G^\circ$ (KJ/mol)	$\Delta H^\circ$ (KJ/mol)	$\Delta S^\circ$ (KJ/mol)
313	- 862.574	0.3046	2.7568
323	-890.142		
333	-917.709		
343	-945.278		

#### Kinetics of the biosorption

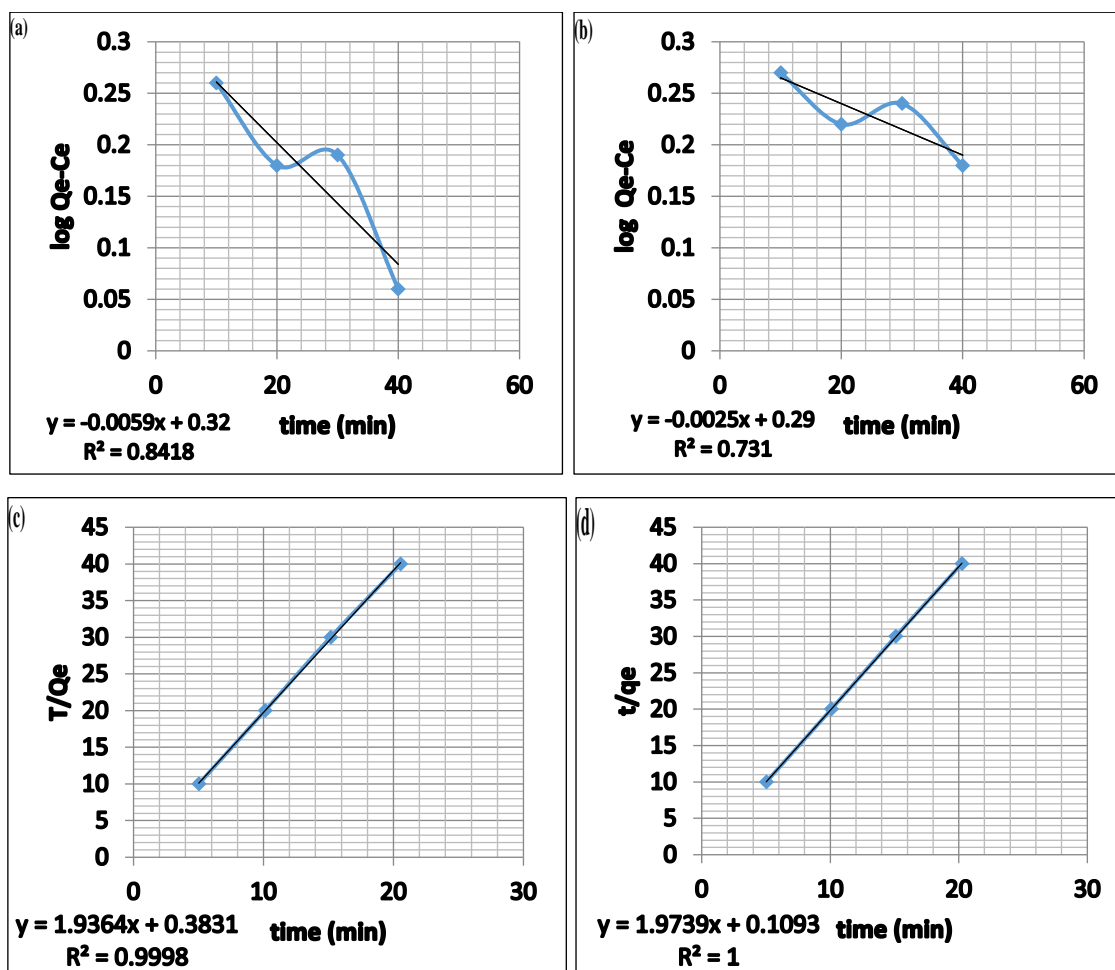
Two kinetic models; first order and second order were used to describe the experimental data obtained for the adsorption of antimony onto tea leaves and tea fiber. The correlation coefficient ( $R^2$ ) was 0.842 and 0.731 for both tea leaves and tea fiber for the first order. On the other hand, the value of  $R^2$  for the second order was 1.00, for tea leaves and tea fiber respectively (figure 7), which both agree well with the experiment data. The second-order kinetics model better describes antimony adsorption on tea leaves and fiber, indicating chemisorption due to electron sharing between the adsorbent surface and adsorbate. Tables 5 and 6 show data for first and second-order kinetic models for antimony sorption by tea leaves and fibers. Second-order kinetics were better, while first-order kinetics had a large deviation.

Table 5. First-order kinetics for both tea leaves and tea fibers

Tea leaves			Tea fibers		
Time (min)	a-x	K1	Time (min)	a-x	K1
10	38.0085	10.3836	10	38.0075	10.3782
20	38.024	5.2336	20	38.017	5.2146
30	38.0205	3.4827	30	38.0125	3.4685
40	38.0535	2.6574	40	38.024	2.6168

**Table 6.** Second-order kinetics for both tea leaves and tea fibers

Time (min)	a-x	x	K1	Time (min)	a-x	x	K1
10	38.0085	1.9915	0.01309	10	38.0075	1.9925	0.0131
20	38.024	1.976	0.01299	20	38.017	1.983	0.0260
30	38.0205	1.9795	0.03905	30	38.0125	1.9875	0.0392
40	38.0535	1.9465	0.2046	40	38.024	1.976	0.0519



**Fig. 7.** First-order (a, b) and second-order (c, d) kinetic studies of tea leaves (a, c) and tea fibers (b, d). (c)

## CONCLUSIONS

In this study, tea leaves and tea fiber were investigated for adsorption of antimony from an aqueous medium and were found to be effective biosorbent for the removal of Sb (II) from simulated wastewater, the study showed that the different parameters observed during the research including initial concentration, contact time, the adsorbent dose, temperature, and pH of the solution influenced the adsorption process. Two adsorption isotherms, namely, Langmuir and Freundlich were used to analyze data. The Langmuir isotherm gives the following correlation coefficient  $R^2$  values of 0.7831 and 0.2519 for tea leaves and tea fiber respectively. In contrast, the Freundlich isotherm gives 0.3607 and 0.8265 values for tea leaves and fiber, respectively. The kinetic study utilized first-order and second-order kinetics, with the second order fitting well for tea leaves and fiber. Thermodynamic studies confirmed a feasible, spontaneous, and endothermic adsorption process. The research suggests that low-cost by-products of tea leaves and fiber processing can effectively remove antimony from wastewater.

## REFERENCES

- [1] TRUEBY, P. Impact of Heavy Metals on Forest Trees from Mining Areas (2003).

- [2] NUSSEY, G., Metal ecotoxicology of the upper Olifants River at selected localities and the effect of copper and zinc on fish blood physiology. Ph.D-thesis, Rand Afrikaans University, South Africa (1998).
- [3] BRADL H., Heavy Metals in the Environment: Origin, Interaction and Remediation Volume 6. London: Academic Press. [Google Scholar]
- [4] PENG, L., WANG, N., XIAO, T., WANG, J., QUAN, H., FU, C., KONG, Q., ZHANG, X., Chemosphere, 327, 2023, <https://doi.org/10.1016/j.chemosphere.2023.138529>.
- [5] BARRERA, H., URENA-NUNEZ, F., BILYEU, B., DIAZ, C.B., J. Hazard. Matter., 146, no. 3, 2006, p. 270, <https://doi.org/10.1016/J.JHAZMAT.2006.01.021>.
- [6] HYLANDER, L.D., MEILI, M., Sci. Total Environ., 304, no. 1-3, 2003, p. 13, [https://doi.org/10.1016/S0048-9697\(02\)00553-3](https://doi.org/10.1016/S0048-9697(02)00553-3).
- [7] JÄRUP, L., Br. Med. Bull., 68, 2003, p. 167, <https://doi.org/10.1093/bmb/ldg032>.
- [8] ŞEKER, A., SHAHWAN, T., EROĞLU, A.E., YILMAZ, S., DEMIREL, Z., DALAY, M.C., J. Hazard. Mat., 154, 2008, p. 973, <https://doi.org/10.1016/J.JHAZMAT.2007.11.007>.
- [9] NAIYA, T. K., BHATTACHARYA, A. K., MANDAL, S., DAS, S. K., J. Hazard. Mat., 163, no. 2-3, 2009, p. 1254, <https://doi.org/10.1016/j.jhazmat.2008.07.119>.
- [10] APPELO, C.A.J., POSTMA, D., Geochemistry, Groundwater and Pollution (2nd ed.). CRC Press., 2005, <https://doi.org/10.1201/9781439833544>.
- [11] EDDY, N.O., UKPE, R.A., GARG, R., GARG, R., ODIONENYI. A.O., AMEH, P., AKPET, I.N., Int. J. Environ. Anal. Chem., 2024, <https://doi.org/10.1080/03067319.2023.2295934>.
- [12] MAFTOUH, A., EL FATNI, O., EL HAJJAJI, S., JAWISH, M.W., SILLANPAA, M., Biointerface Res. App. Chem., 13, no. 4, 2023, p. 397, <https://doi.org/10.33263/BRIAC134.397>.
- [13] SALEH, T.A., Environ. Technol. Innov., 24, 2021, <https://doi.org/10.1016/j.eti.2021.101821>.
- [14] IQBAL, M., SAEED, A., EDYVEAN, R.G.J., Chem. Eng. J., 225, 2013, p. 192, <https://doi.org/10.1016/j.cej.2013.03.079>.
- [15] ULUOZLU, O.D., SARI, A., TUZEN, M., Chem. Eng. J., 163, 2010, p. 382, <https://doi.org/10.1016/j.cej.2010.08.022>.
- [16] HASAN, M.B., AL-TAMEEMI, I.M., ABBAS, M.N., J. Ecol. Eng., 22, 2021, p. 25, <https://doi.org/10.12911/22998993/130632>.
- [17] PRADHAN, S., SINGH, S., RAI, L.C., Bioresour. Technol., 98, no. 3, 2007, p. 595, <https://doi.org/10.1016/j.biortech.2006.02.041>.
- [18] MANN, S., MANDA, A., Int. J. Engine. Res. Appl., 4, no. 7, 2014, p. 116, [www.ijera.com](http://www.ijera.com).
- [19] YAKUBU, S., ETIM, E.E., J. Chem. React. Synth., 13, no. 2, 2023, p. 129, [https://journals.iau.ir/article\\_704705\\_8078ec4646f641150ecc3dadbe509989.pdf](https://journals.iau.ir/article_704705_8078ec4646f641150ecc3dadbe509989.pdf).
- [20] ETIM, E. E., ETIOWO, G., U., EFFIONG, O. E., GODWIN, O. E., Int. J. Adv. Res. Chem. Sci., 6, no. 9, 2019, p. 20, <http://dx.doi.org/10.20431/2349-0403.0609003>.
- [21] REDDAD, Z., GERENTE, C., ANDRES, Y., LE CLOIREC, P., Environ. Sci. Technol., 36, no. 9, 2002, p. 2067, <https://doi.org/10.1021/es0102989>.
- [22] KHALAF, M.A., Bioresour. Technol., 99, no. 14, 2009, p. 6631, <https://doi.org/10.1016/j.biortech.2007.12.010>.
- [23] KUYUCAK, N., VOLESKY, B., Biotechnol. Lett., 10, 1988, p. 137, <https://doi.org/10.1007/BF01024641>.
- [24] ETIM, E.E., YAKUBU, S., GRACE, S., OGOFOHTA, G.O., FUW Trends in Science & Technology Journal, 7, no.3, 2022, p. 203, <https://ftstjournal.com/uploads/docs/73%20Article%2030%20pp%20203-218.pdf>.
- [25] REHMAN, H., SHAKIRULLAH, M., AHMAD I., SHAN, S., HAMEEDULLAH, J. Chin. Chem. Soc., 53, no. 5, 2006, p. 1045, <https://doi.org/10.1002/jccs.200600139>.
- [26] VASUDEVAN, P., PADMAVATHY, V., DHINDRA, S.C., Bioresour. Technol., 89, no. 3, 2003, p. 281, [https://doi.org/10.1016/S0960-8524\(03\)00067-1](https://doi.org/10.1016/S0960-8524(03)00067-1)
- [27] XU, L., PAPANIKOLAOU, K.G., LECHNER, B., JE, L., SAMORJAI, G., SALMERON, M., MAVRIKAKIS, M., Science, 380, 2023, p. 70, <https://doi.org/10.1126/science.add0089>.

- [28] BABARINDE, N.A.A., OYEBAMIJI BABALOLA, J., ADEBOWALE SANNI, R., *Int. J. Phys. Sci.*, 1, no. 1, 2006, p. 23, <https://doi.org/10.5897/IJPS.9000097>.
- [29] PAVASANT, P., APIRATIKUL, R., SUNGKHUM, V., SUTHIPARINYANONT, P., WATTANACHIRA, S., MARHABA, T., *Bioresour. Technol.*, 97, no. 18, 2006, <https://doi.org/10.1016/j.biortech.2005.10.032>.
- [30] FEBRIANTO, J., KOSASIH, A.N., SUNARSO, J., JU, Y.H., INDRASWATI, N., ISMADJI, S., *J. Hazard. Mater.*, 162, no. 2-3, 2009, p. 616, <https://doi.org/10.1016/j.jhazmat.2008.06.042>.
- [31] HO, S.N., BIGGAR, S.R., SPENCER, D.M., SCHREIBER, S.L., CRABTREE, G.R., *Nature*, 382, 1996, p. 822, <https://doi.org/10.1038/382822a0>.
- [32] HO, Y.S., MCKAY, G., *Adsorp. Sci. Technol.*, 20, 2002, p. 797, <http://dx.doi.org/10.1260/026361702321104282>.
- [33] SHAIK BASHA, S., MURTHY, Z.V.P., JHA, B., *Ind. Eng. Chem. Res.*, 47, no. 3, 2008, p. 980, <https://doi.org/10.1021/ie071210o>.
- [34] ABDEL-GHANI, N., HEGAZY, A., EL-CHAGHABY, G., *Int. J. Environ. Sci. Technol.*, 6, 2009, p. 243, <https://doi.org/10.1016/J.DESAL.2009.02.065>.
- [35] VOUDRIAS, E., FYTIANOSAND, F., BOZANI, E., *Global Nest. Int. J.*, 4, no. 1, 2002, p. 75, <https://doi.org/10.30955/gnj.000233>.
- [36] DADA, A.O., OLALEKAN, A.P., OLATUNYA, A.M., DADA, O., *IOSR J. Appl. Chem.*, 3, 2012, p. 38, <http://dx.doi.org/10.9790/5736-0313845>.
- [37] WANG, Y., ZHAO, A., JI, G., ZHANG, H., *Environ. Geochem. Health*, 28, 2006, <https://doi.org/10.1007/s10653-005-9023-z>.
- [38] TEMKIN, M., PYZHEV, J.A.V., *ActaPhysiochem.*, 12, 1940, p. 217.
- [39] DEMIRBAS, O., ALKAN, M., DOĞAN, M., *Adsorption*, 8, 2002, p. 341.
- [40] AKSU, Z., *Process Biochem.*, 40, 2005, p. 997, <http://dx.doi.org/10.1016/j.procbio.2004.04.008>.
- [41] BABALOLA, J.O., BAMIDELE, T.M., ADENIJI, E.A., ODOZI, N.W., OLATUNDE, A.M., OMOROGIE, M.O., *Model. Earth Syst. Environ.*, 2, 2016, p. 1, <https://doi.org/10.1007/s40808-016-0246-z>.
- [42] MALANDRINO, M., ABOLLINO, O., GIACOMINO, A., ACETO, M., MENTASTI, E., *J. Colloid Interface Sci.*, 299, no. 2, 2006, p. 537, <https://doi.org/10.1016/j.jcis.2006.03.011>.
- [43] SHUKLA, S.R., PAI, R.S., *Sep. Purif. Technol.*, 43, 2005, p. 1, <https://doi.org/10.1016/J.SEPPUR.2004.09.003>.
- [44] LIU, H.Y., CHEN, B.Y., LAN, Y.W., CHENG, Y.C., *Chem. Eng. J.*, 97, no. 2–3, 2004, p. 195, [https://doi.org/10.1016/S1385-8947\(03\)00210-9](https://doi.org/10.1016/S1385-8947(03)00210-9).

Citation: Etim, E.E., Yakubu, S., Okafor, R., Bako, B, Biosorption of antimony using tea leaves and tea fibers (*Camellia sinensis*) as adsorbents: thermodynamics, isotherm, and kinetics, *Rom. J. Ecol. Environ. Chem.*, 2024, 6, no.1, pp. 33–45.



© 2024 by the authors. This article is an open access article distributed under the terms and conditions of the Creative Commons Attribution (CC BY) license (<http://creativecommons.org/licenses/by/4.0/>).